Digestive Diseases and Sciences (2018) 63:2639–2650
https://doi.org/10.1007/s10620-018-5053-0

ORIGINAL ARTICLE

Regulation of Autophagy Affects the Prognosis of Mice with Severe Acute Pancreatitis

Jianhua Wan[1] · Jie Chen[1] · Dangyan Wu[1] · Xiaoyu Yang[1] · Yaobin Ouyang[1] · Yin Zhu[1] · Liang Xia[1] · Nonghua Lu[1]

Received: 12 June 2017 / Accepted: 31 March 2018 / Published online: 9 April 2018

Abstract

Background Acute pancreatitis (AP) is a common inflammatory disease that may develop to severe AP (SAP), resulting in life-threatening complications. Impaired autophagic flux is a characteristic of early AP, and its accumulation could activate oxidative stress and nuclear factor κB (NF-κB) pathways, which aggravate the disease process.

Aim To explore the therapeutic effects of regulating autophagy after the onset of AP.

Methods In this study, intraperitoneal injections of 3-methyladenine (3-MA) and rapamycin (RAPA) in the L-arginine or cerulein plus lipopolysaccharide (LPS) Balb/C mouse model. At 24 h after the last injection, pulmonary, intestinal, renal and pancreatic tissues were analyzed.

Results We found that 3-MA ameliorated systemic organ injury in two SAP models. 3-MA treatment impaired autophagic flux and alleviated inflammatory activation by modulating the NF-κB signaling pathway and the caspase-1-IL-1β pathway, thus decreasing the injuries to the organs and the levels of inflammatory cytokines.

Conclusion Our study found that the regulation of autophagy could alter the progression of AP induced by L-arginine or cerulein plus LPS in mice.

Keywords Acute pancreatitis · Autophagy · 3-methyladenine · Inflammatory

Abbreviations

AP	Acute pancreatitis
SAP	Severe AP
NF-κB	Nuclear factor κB
IP	Intraperitoneal
3-MA	3-methyladenine
RAPA	Rapamycin
LPS	Lipopolysaccharide
LC3-II	Microtubule-associated protein 1 light chain 3
ZO-1	Zonula occludens-1
IHC	Immunohistochemistry
LDH	Lactate dehydrogenase
ELISA	Enzyme-linked immunosorbent assay
BCA	Bicinchoninic acid
SDS	Sodium dodecyl sulfate
PVDF	Polyvinylidene fluoride
ECL	Enhanced chemiluminescence
JAM	Junctional adhesion molecules

Electronic supplementary material The online version of this article (https://doi.org/10.1007/s10620-018-5053-0) contains supplementary material, which is available to authorized users.

Liang Xia and Nonghua Lu equal contribution by the corresponding authors.

✉ Liang Xia
xialiang79@163.com

✉ Nonghua Lu
lunonghua@ncu.edu.cn

Jianhua Wan
18942337437@163.com

Jie Chen
18270916863@163.com

Dangyan Wu
wudangyan00@163.com

Xiaoyu Yang
18720998268@163.com

Yaobin Ouyang
18720997548@163.com

Yin Zhu
zhuyin27@sina.com

[1] Department of Gastroenterology, The First Affiliated Hospital of Nanchang University, 17 Yongwaizheng Street, Nanchang 330006, Jiangxi, People's Republic of China

ALI Acute lung injury
PI3K Phosphatidylinositol 3-kinase
ROS Reactive oxygen species

Introduction

Acute pancreatitis (AP) is an inflammatory condition of the pancreas that is not confined only to the pancreas parenchyma but also frequently combined with a systemic inflammatory response. Although mild AP always presents as a self-limiting disorder in a majority of AP patients, some patients develop severe AP (SAP), which is characterized with pancreatic necrosis, systemic inflammatory response syndrome, multiple organ failure, sepsis and mortality [1]. Recent studies have revealed that SAP begins with the activation of zymogens in pancreatic acinar cells, dysregulation of multiple signaling pathways, release of pro-inflammatory cytokines and chemokines, induction of local and systemic inflammatory responses and pancreatic necrosis through acinar cell death [2]. Treatments for SAP have had rapidly developed during recent years, but mortality from SAP has not been significantly decreased. Thus, the development of specific pharmacotherapies to treat or prevent the progression of SAP by clarifying the complex disease pathogenesis is urgently needed.

Autophagy is a lysosomal degradation pathway that recycles organelles and long-lived proteins. In most cells, autophagy is a major protective mechanism that enables cell survival and adaptation to fluctuations in environmental conditions. In the physiological state, the pancreas exhibits a high rate of zymogen synthesis, and thus, there is an increased need to remove defective or excessive proteins by autophagy [3]. In AP, autophagic flux is impaired, causing an accumulation of autolysosomes in acinar cells, which exhibit increased levels of the lysosomal markers microtubule-associated protein 1 light chain 3 (LC3-II) and p62/sequestosome 1 (SQSTM1) [4]. Impaired autophagy could increase the accumulation of reactive oxygen species (ROS) due to defective clearance of damaged or depolarized mitochondria and activate oxidative stress and nuclear factor κB (NF-κB) pathways to aggravate the disease process. Thus, effective intervention of autophagy is expected to be a means to reduce the progression of pancreatitis.

So far, very few studies of AP have addressed the role of autophagy in vivo. *Yang et al.* reported that NF-κB pathway activation stimulates autophagy during sodium taurocholate-induced acute necrotizing pancreatitis in rats [5]. However, the regulation of autophagy to ameliorate injury in pancreatic acinar cells during SAP and whether it can affect the prognosis of SAP in mice has not yet been elucidated. This study was designed to investigate the regulation of autophagy in two SAP experimental models generated by the administration of L-arginine or cerulein combined with lipopolysaccharide (LPS) in mice.

Materials and Methods

Reagents

Cerulein (Catalog No. C9026), LPS (Catalog No. L4130), L-arginine (Catalog No. A5006), 3-methyladenine (3-MA) (Catalog No. M9281) and rapamycin (RAPA) (Catalog No. PHZ1235) were purchased from Sigma-Aldrich (St. Louis, MO, USA). The primary antibodies used for immunoblotting were as follows: P62 (Catalog No. 5114), IL-1B caspase-1 (Catalog No. 2225), IκBα (Catalog No. 9242), beclin-1 (Catalog No. 3738) and p-p65 (Ser536) (Catalog No. 3031) purchased from Cell Signaling Technology (Danvers, MA, USA); and occludin (Catalog No. 71-1500) and zonula occludens-1 (ZO-1) (Catalog No. 40-2200) purchased from Life Technologies Inc. The primary antibodies used for immunohistochemistry (IHC) were LC3 purchased from Sigma-Aldrich and beclin-1 (Catalo No. ab62557), p65 (Catalo No. ab16502), myeloperoxidase (MPO) (Catalo No. ab134132), caspase-1 (Catalo No. ab1872), IκBα (Catalo No. ab32518), p-p65 (phospho S536) (Catalo No. ab86299) and claudin-4 (Catalo No. ab15104) purchased from Abcam (Inc., Cambridge, MA, USA). Amylase assay kits (C016-1), lipase assay kits (A054-2), lactate dehydrogenase (LDH) assay kits (A020-2) and myeloperoxidase assay kits (A044) were purchased from Nanjing Jiancheng Bioengineering Institute (Jiancheng Biotech, Nanjing, China).

Mice

Male BALB/C mice (25 ± 3 g; 6–8 weeks old) were purchased from Hunan SJA Laboratory Animal Co., Ltd. (HSLAC, Hunan, China). All animals were housed in an environmentally controlled room (22 ± 2 °C; 50% relative humidity; 12-h light/dark cycle). After 1 week of acclimatization, the mice were deprived of food 12 h before the experiments but had free access to water. All animal experiments were approved by the Institutional Animal Care and Use Committee of The First Affiliated Hospital of Nanchang University and performed in accordance with the guidelines of the Animal Care and Use Committee.

Experimental Design

Two SAP models were applied in this study. Cerulein pancreatitis was induced as previously described [6]. Briefly, mice were treated by 10 h intraperitoneal (IP) injections of a supramaximal dose of cerulein (100 μg/kg). The cerulein plus LPS model was induced by IP injection of

lipopolysaccharide (5 mg/kg) immediately after the 10-h IP injections of a supramaximal dose of cerulein (100 μg/kg). Mice were killed 24 h after the last cerulein injection. Arginine pancreatitis was induced as previously described [7]. Mice were IP injected twice with L-arginine solution (8%, pH = 7.4) at an interval of 1 h and a dose of 4 g/kg. The mice were killed 24 h after the last L-arginine injection. An equal amount of saline was injected into the control mice. Cerulein, LPS and L-arginine were dissolved in saline solution. A total of 8–12 mice were randomly assigned to each group. Serum as well as pulmonary, intestinal, renal and pancreatic tissues was obtained for subsequent analyses.

Drug Treatment

SAP was induced by L-arginine or cerulein plus LPS. 3-MA (10 or 20 mg/kg), and RAPA (2 or 4 mg/kg) was administered by IP injection 2 h after the last LPS or L-arginine injection. Mice were killed 24 h after the last cerulein or L-arginine injection. Blood samples were taken for the analysis of cytokine and enzyme levels. Pulmonary, intestinal, renal and pancreatic tissue was rapidly removed and fixed in formalin for subsequent analyses.

Histological Analysis

Fresh specimens of mice were fixed in 10% formalin for over 24 h, embedded in paraffin, and cut into 4-mm-thick sections, which were processed for hematoxylin and eosin (H&E) staining. The morphological changes were observed under a microscope by two pathologists in a blinded manner. An assessment of vacuolization, edema, acinar cell necrosis and inflammatory cell infiltration was carried out. Pancreatic injury was scored on a scale of 0–3 according to four items: edema (0 absent, 1 focally increased between lobules and 2 diffusely increased); inflammatory cell infiltrate (0 absent, 1 in ducts (around ductal margins), 2 in the parenchyma (< 50% of the lobules) and 3 in the parenchyma (> 50% of the lobules)); hemorrhage and fat necrosis (0 absent, 1 (1–2 foci), 2 (3–4 foci), 3 (> 5 foci)); and acinar necrosis (0 absent, 1 periductal necrosis (< 5%), 2 focal necrosis (5–20%) and 3 diffuse parenchymal necrosis (20–50%)), as previously described [8, 9].

Measurements of Serum Cytokine, Amylase, Lipase, MPO and LDH Activity

Blood was collected by cardiac puncture and centrifuged at 3000 rpm for 10 min to collect serum. The levels of serum cytokines, including TNF-α, IL-1β, IL-6, IL-10 and IL-17, in murine serum were analyzed using a commercially available enzyme-linked immunosorbent assay (ELISA) kit (eBioscience, San Diego, CA, USA) according to the manufacturer's instructions. The serum activities of amylase and lipase were measured using a commercially available kit (Jiancheng Biotech, Nanjing, China) and expressed as units per liter (U/L). Enzyme activity was determined using MPO and LDH detection kits according to the manufacturer's instructions (Jiancheng Biotech, Nanjing, China).

Electron Microscopy

The pancreatic tissues were cut to a suitable size (approximately $1 \times 1 \times 1$ mm^3) in 2% glutaraldehyde buffer and then post-fixed with 2% osmium tetroxide. Ultrathin sections (70 nm) were sectioned using a microtome. The sections were viewed by electron microscopy (JEM 1230, JEOL, Tokyo, Japan) to determine changes in the pancreatic acinar autophagic vacuoles.

Immunohistochemistry

Pancreatic and pulmonary tissues of mice were taken and immediately fixed in 10% buffered formalin for over 24 h, dehydrated by an automatic tissue hydroextractor, embedded in paraffin and cut into 4-mm sections. After blocking endogenous peroxidase with 3% H_2O_2 for 8 min, the sections were incubated overnight with primary antibodies. Then, the sections were incubated in secondary antibodies, developed with 3,3-diaminobenzidine (DAB) solution and counterstained with hematoxylin. Negative controls were established using rabbit IgG instead of primary antibodies. The sections were observed by light microscopy at a magnification of ×200 (CKX41, Olympus, Tokyo, Japan). The histological sections were evaluated by two experienced pathologists, and the degree of staining was scored as follows: 0 (0%), 1 (1–25%), 2 (26–50%), 3 (51–75%) and 4 (76–100%) for positive staining; and 0 (normal), 1 (weak), 2 (medium) and 3 (strong) for the staining intensity [10].

Western Blotting

Total protein was extracted from the pancreatic tissues of mice by centrifugation. Protein concentrations were quantified using the bicinchoninic acid (BCA) protein assay (Tiangen, Beijing, China). Proteins were separated by sodium dodecyl sulfate (SDS)-polyacrylamide gel electrophoresis and then transferred to a polyvinylidene fluoride (PVDF) membrane. After blocking with 2% bovine serum albumin (BSA), the membranes were immunoblotted with the indicated primary antibodies (including anti-LC3, anti-p62, anti-beclin-1, anti-ubiquitin, anti-phos-p65 and anti-NF-κb p65) and then with HRP-conjugated secondary antibody for 4 h at 4 °C. The proteins were visualized using an enhanced chemiluminescence (ECL) system (Thermo Scientific).

Statistical Analysis

The data are expressed as the mean ± SEM. Statistical analyses, including the Mann–Whitney nonparametric *U* test and 2-tailed Student's *t* test, were performed using SPSS statistical software 20.0 (IBM Corp., Armonk, NY, USA). In all cases, P values < 0.05 were considered to be statistically significant.

Results

3-MA and RAPA Affected Serum Amylase and Lipase Levels as well as Induced Histopathological Alterations of the Pancreas in Cerulein Plus LPS-Induced SAP Mice

The model of SAP induced by cerulein combined with LPS had been shown in previous studies [6]. The autophagy-regulating compounds 3-MA and RAPA were administered by IP injection 2 h after the last injection of LPS (Fig. 1a). Mortality in the cerulein plus LPS group at 24 h was 36%

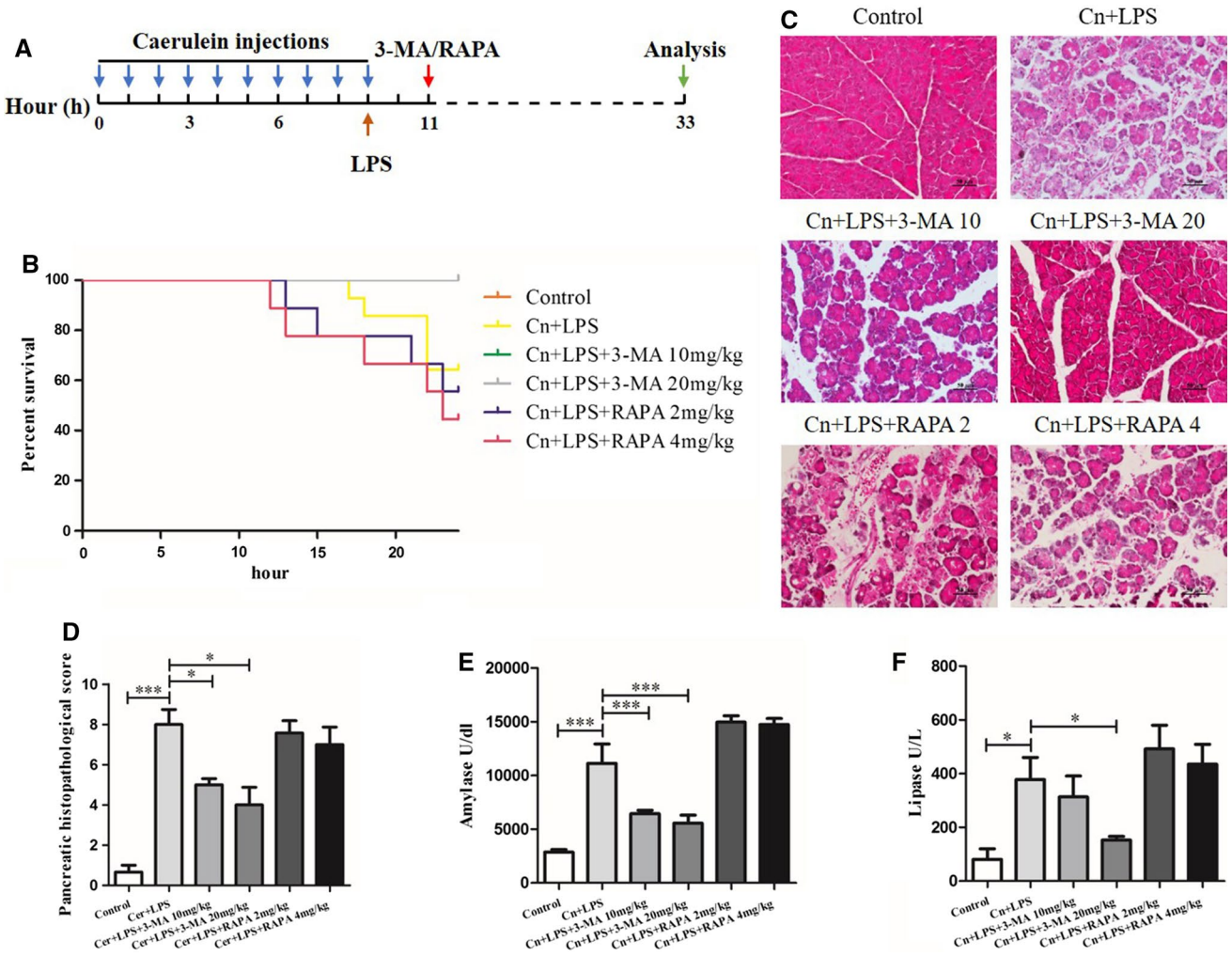

Fig. 1 The autophagy-regulating compounds affected the severity of SAP in cerulein plus LPS-induced mice. **a** SAP was induced in BABL/c mice with a high dose of cerulein (100 μg/kg × 10) plus LPS (5 mg/kg), and the autophagy-regulating compounds 3-MA (10 or 20 mg/kg) and RAPA (2 or 4 mg/kg) were intraperitoneally administered 2 h after the last injection of LPS. The mice were killed under anesthesia at 24 h after the last injection of LPS. **b** The survival rate of each group at different time points during the 24 h after the last injection of LPS. **c** H&E staining of pancreas tissue from each group indicated different tissue injuries, including pancreatic edema, extravascular infiltration and acinar cell necrosis (×200). **d** Histopathological score of pancreatitis severity. **e**, **f** Serum amylase (U/L) and serum lipase (U/L) activity. Each value represents the mean ± standard deviation ($n = 8$–12 per group). $^{*}P < 0.05$, $^{**}P < 0.01$, and $^{***}P < 0.001$

(5/14) versus 44% (4/9) and 55% (5/9) in the 2 and 4 mg/kg RAPA groups, respectively. However, all animals in the control and the two 3-MA groups survived at 24 h compared with the untreated cerulein plus LPS mice ($P < 0.05$) (Fig. 1b). Compared with the normal pancreas, histological examination of the pancreas after cerulein plus LPS induction showed tissue injury characterized by marked edema, inflammatory cell infiltration and a large number of necrotic acinar cells (Fig. 1c, d). Necrosis of the pancreatic acinar cells and inflammatory cell infiltration were significantly reduced in the 3-MA-treated cerulein plus LPS mice compared with the untreated cerulein plus LPS mice. In contrast, the pathological damage in the pancreatic tissues was still very serious following treatment with RAPA (Fig. 1c, d). At both doses, 3-MA significantly ameliorated the decrease in serum amylase and lipase activity compared to the untreated cerulein plus LPS mice; however, both doses of RAPA led to elevated serum amylase and lipase activity compared to the untreated cerulein plus LPS mice (Fig. 1e).

Levels of Serum Cytokines and LDH After Regulating Autophagy in Cerulein Plus LPS-Induced SAP Mice

Serum cytokine levels reflect the severity of inflammation and can predict prognosis in cases of human AP [11]. Pro-inflammatory cytokines, such as TNF-α, IL-1β, IL-6, IL-10 and IL-17, play key roles in the pathogenesis of SAP [12–14]. In cerulein plus LPS mice, those inflammatory cytokines, including TNF-α, IL-1β, IL-6, IL-10 and IL-17, were significantly increased compared to the control mice ($P < 0.01$) (Fig. 2a). When the cerulein plus LPS mice were treated with a high dose of 3-MA, the levels of IL-1β, IL-6 and IL-17 were significantly decreased compared to the untreated cerulein plus LPS mice ($P < 0.05$) (Fig. 2a). IL-10, a cytokine synthesis inhibitory factor, was significantly increased following treatment with 3-MA ($P < 0.05$) (Fig. 2a). However, the level of IL-1β was higher in the RAPA group than other groups ($P < 0.05$) (Fig. 2a). LDH activity was examined to evaluate the degree of pancreatic acinar cell necrosis [15]. Mice with cerulein plus LPS showed increased LDH activity in the serum and pancreas; however, 3-MA significantly reduced LDH activity (Fig. 2b, c).

3-MA Inhibited Autophagy and Pancreatic Inflammation as well as Down-Regulated NF-κB Signaling in Cerulein Plus LPS Mice

Transmission electron microscopy, an important technique for the observation autophagy, revealed autophagic vacuoles in the activated autophagy samples. The percentage of autophagic vacuoles per cytoplasmic area was significantly increased in the cerulein plus LPS group compared with that in the control group. However, the administration of 3-MA significantly decreased the percentage of autophagic vacuoles per cytoplasmic area compared with the cerulein plus LPS group (Fig. 3a). To determine whether autophagy was over-activated, the expression levels of autophagy proteins beclin-1 and LC3I/II were detected by immunohistochemistry and western blotting. The level of beclin-1, p62 and LC3II expression was significantly increased in the cerulein plus LPS group compared with that in the control group, as determined by immunoblotting (Fig. 3b and Sup Fig. 1). Excessive cell vacuolization and accumulation

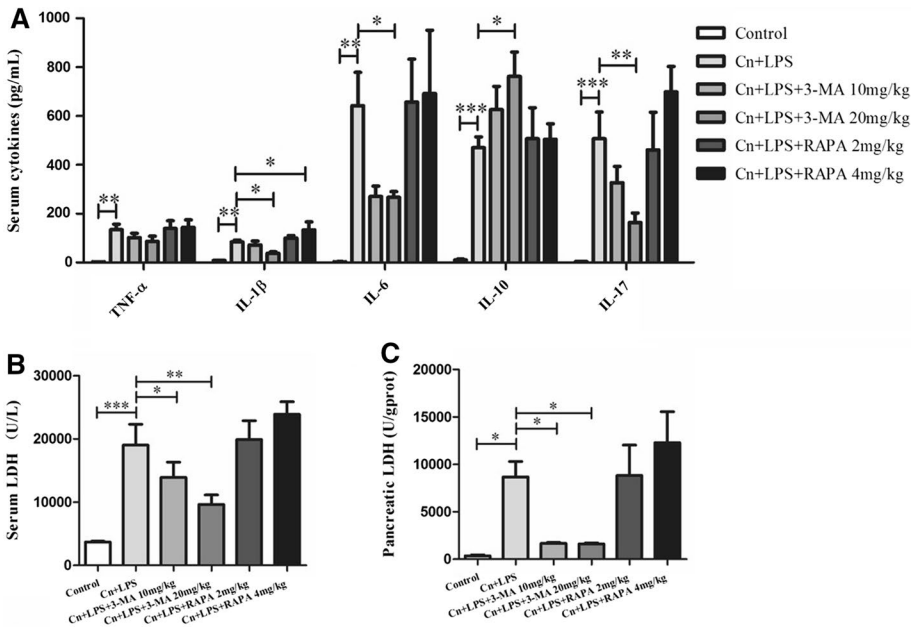

Fig. 2 Levels of serum cytokines and LDH after modulating autophagy in cerulein plus LPS mice. **a** ELISA was used to determine the levels of serum TNF-α, IL-1β, IL-6, IL-10 and IL-17 (pg/mL) in each treatment group. **b**, **c** Serum LDH (U/L) and pancreatic LDH (U/gprot). Each value represents the mean ± standard deviation ($n = 8$–12 per group). $^{*}P < 0.05$, $^{**}P < 0.01$, and $^{***}P < 0.001$

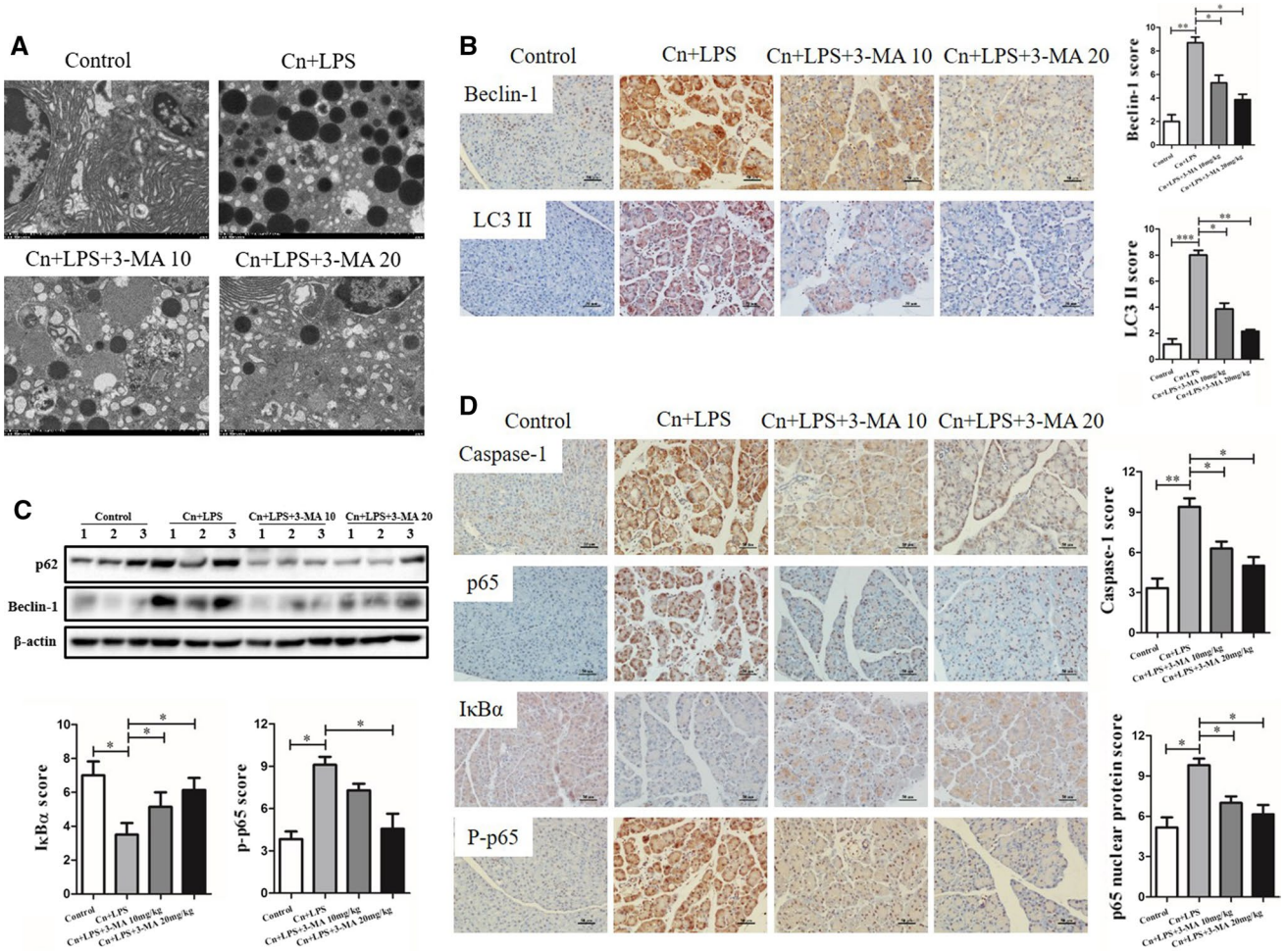

Fig. 3 3-MA treatment ameliorated pancreatic inflammation and reduced NF-κB signaling in cerulein plus LPS mice. **a** Autophagic vacuoles were detected in pancreatic tissue samples by transmission electron microscopy (TEM) (×10,000). Two different doses of 3-MA reduced the formation of autophagic vacuoles compared to the untreated cerulein plus LPS group. **b** Immunohistochemical evaluation revealed the effect of the two 3-MA doses on autophagy by revealing the expression levels of beclin-1 and LC3 II in the pancreas (×200). The immunohistochemical scores of beclin-1 and LC3 II staining were analyzed. **c** Protein expression of p62 and beclin-1 was determined by western blotting, and the gray values were calculated. **d** Immunohistochemical evaluation of pancreatic inflammation and NF-κB signaling in the mice treated with two different doses of 3-MA, revealing the expression levels of caspcase-1, IκBα, p65 nuclear protein and phosphorylated-p65 in the pancreas (×200). The immunohistochemical scores of caspcase-1, IκBα, p65 nuclear protein and phosphorylated-p65 were analyzed. Each value represents the mean ± standard deviation ($n = 8$–12 per group). $^{*}P < 0.05$, $^{**}P < 0.01$ and $^{***}P < 0.001$

of p62 together with LC3-II are markers of impaired autophagy. In addition, the administration of 3-MA significantly decreased beclin-1, LC3II and p62 expression compared with untreated cerulein plus LPS mice (Fig. 3b and Sup Fig. 1). Similar expression patterns of beclin-1 and LC3I/II were observed using immunohistochemistry (Fig. 3c). The evaluation of inflammation in the pancreas of cerulein plus LPS mice by immunohistochemistry and/or western blotting revealed elevated expression levels of MPO, caspase-1 and IL-1β in the cerulein plus LPS group compared with that in the control and 3-MA groups (Fig. 3d and Sup Fig. 1). The activation of NF-κB increases the severity of pancreatic inflammatory cascades in cerulein plus LPS mice, and thus, strategies to inactivate NF-κB activity may be used to treat SAP. NF-κB p65 nuclear protein and phosphorylated-p65 expression in the pancreas was significantly increased in cerulein plus LPS mice, and 3-MA treatment reduced the expression of p65 nuclear protein and phosphorylated-p65 (Fig. 3d and Sup Fig. 1). Immunohistochemistry and western blotting showed that the expression of IκBα, the NF-κB inhibitor, was significantly reduced in the cerulein plus LPS group compared the control and 3-MA groups (Fig. 3d and Sup Fig. 1).

3-MA Alleviated Damages of the Lung, Intestine and Kidney in Cerulein Plus LPS-Induced SAP Mice

SAP often causes systemic inflammation that leads to systemic multiple organ dysfunction syndrome, including lung, intestinal and kidney injury [15]. The histological features of lung injury in cerulein plus LPS mice include more obvious thickening of the alveoli, neutrophil infiltration and alveolar congestion than in the control mice. However, treatment of 3-MA at different doses led to markedly reduced pathological characteristics (Fig. 4a). Similarly, the expression levels of MPO in the lung were significantly higher in the cerulein plus LPS mice than in the two 3-MA groups (Fig. 4b). Therefore, 3-MA could be effective for reducing neutrophil transmigration into the lungs. Intestinal barrier function is established by complex junctional structures that are intracellularly connected to zonulins, including the zonula occludens (ZO) family; the tight junctions, which are made up of transmembrane proteins, such as occludin; junctional adhesion molecules (JAM); and claudins. Microscopic morphological evidence of gut injury, including loss of the unstirred mucus layer and neutrophil infiltration, was observed in the cerulein plus LPS group compared to the control group, but 3-MA treatment significantly reduced the damages in the intestine (Fig. 4c). The expression levels of proteins that reflect intestinal barrier function, including occludin, ZO-1 and claudin-4, were significantly lower in the cerulein plus LPS group but were restored in the two 3-MA groups, as determined by western blot and immunohistochemistry (Fig. 4d, e). Light microscopy of kidney tissue in the cerulein plus LPS group revealed renal tubular epithelial cell necrosis, interstitial edema and inflammatory cell infiltration; additionally, 3-MA treatment was effective in reducing the severity of kidney tissue injury (Fig. 4f).

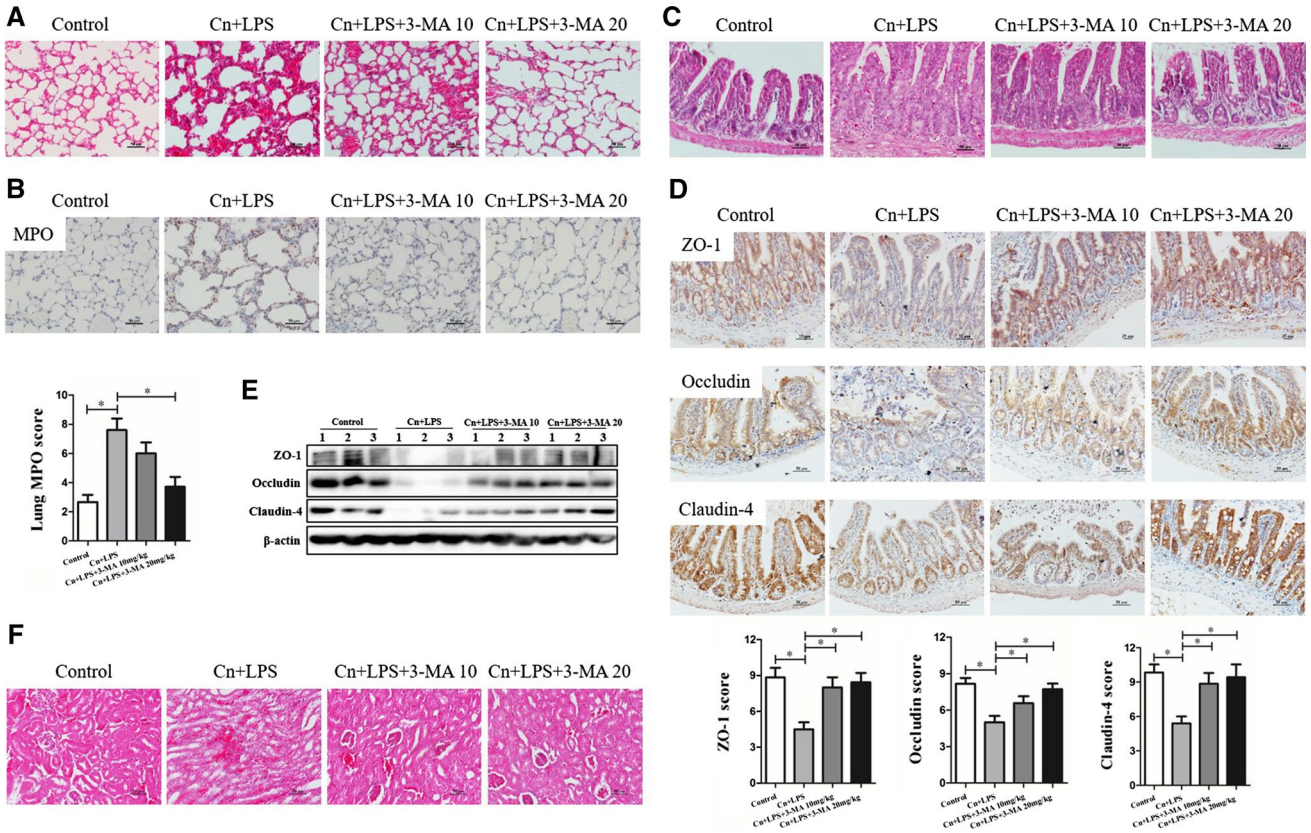

Fig. 4 3-MA treatment alleviated damages in the lung, intestine and kidney of cerulein plus LPS mice. **a** H&E staining of lung samples from the four groups of mice revealed different tissue injuries, including alveolar thickening and inflammation (×200). **b** Immunohistochemical evaluation of inflammation in mice treated with the two doses of 3-MA based on the expression level of MPO in the lung (×200). The immunohistochemical scores of MPO were analyzed. **c** H&E staining of intestinal tissue from the four groups of mice exhibited different tissue injuries, such as disintegration of the lamina propria, crypt layer injury and transmural infarction (×200). **d**, **e** Immunohistochemical and western blotting evaluation of the intestinal barrier function of mice treated with the two doses of 3-MA based on the expression level of occludin, ZO-1 and claudin-4 in the intestine (×200). The immunohistochemical scores of occluding, ZO-1 and claudin-4 were analyzed. **f** H&E staining of kidney tissue from the four groups revealed different tissue injuries, including renal tubular epithelial cells necrosis, interstitial edema, and inflammatory cell infiltration (×200). Each value represents the mean ± standard deviation ($n = 8$–12 per group). $^{*}P < 0.05$, $^{**}P < 0.01$ and $^{***}P < 0.001$

3-MA Could not Reduce the Systemic Inflammatory Response Induced by LPS but Could Significantly Reduce Pancreatic Injury Induced by Cerulein

Next, we identified the role of 3-MA in the model of SAP induced by cerulein combined with LPS administration. Interestingly, the survival rate was lower in the LPS + 3-MA groups than in the LPS group without cerulein (Fig. 5a). The histological features of lung injury in the LPS + 3-MA group included more severe thickening of the alveoli and neutrophil infiltration than in the LPS group (Fig. 5b). The expression levels of MPO in the lung were significantly higher in the LPS + 3-MA group than in the LPS group without cerulein (Fig. 5b). In LPS-induced mice, IL-6 expression was also significantly lower than that in the LPS + 3-MA-treated mice ($P < 0.05$) (Fig. 5c). The level of serum amylase and lipase activity in AP was increased in the cerulein-treated group compared to the control group (Fig. 5d). However, histological examination of the pancreas after cerulein-induction showed tissue injury characterized by mild edema, inflammatory cell infiltration and several necrotic acinar cells; histological examination of the pancreas in the cerulein + 3-MA group revealed that it appeared very similar to that in the control group (Fig. 6e). The percentage of autophagic vacuoles per cytoplasmic area was significantly reduced in the cerulein + 3-MA group compared with the cerulein group (Fig. 6e). In AP-treated

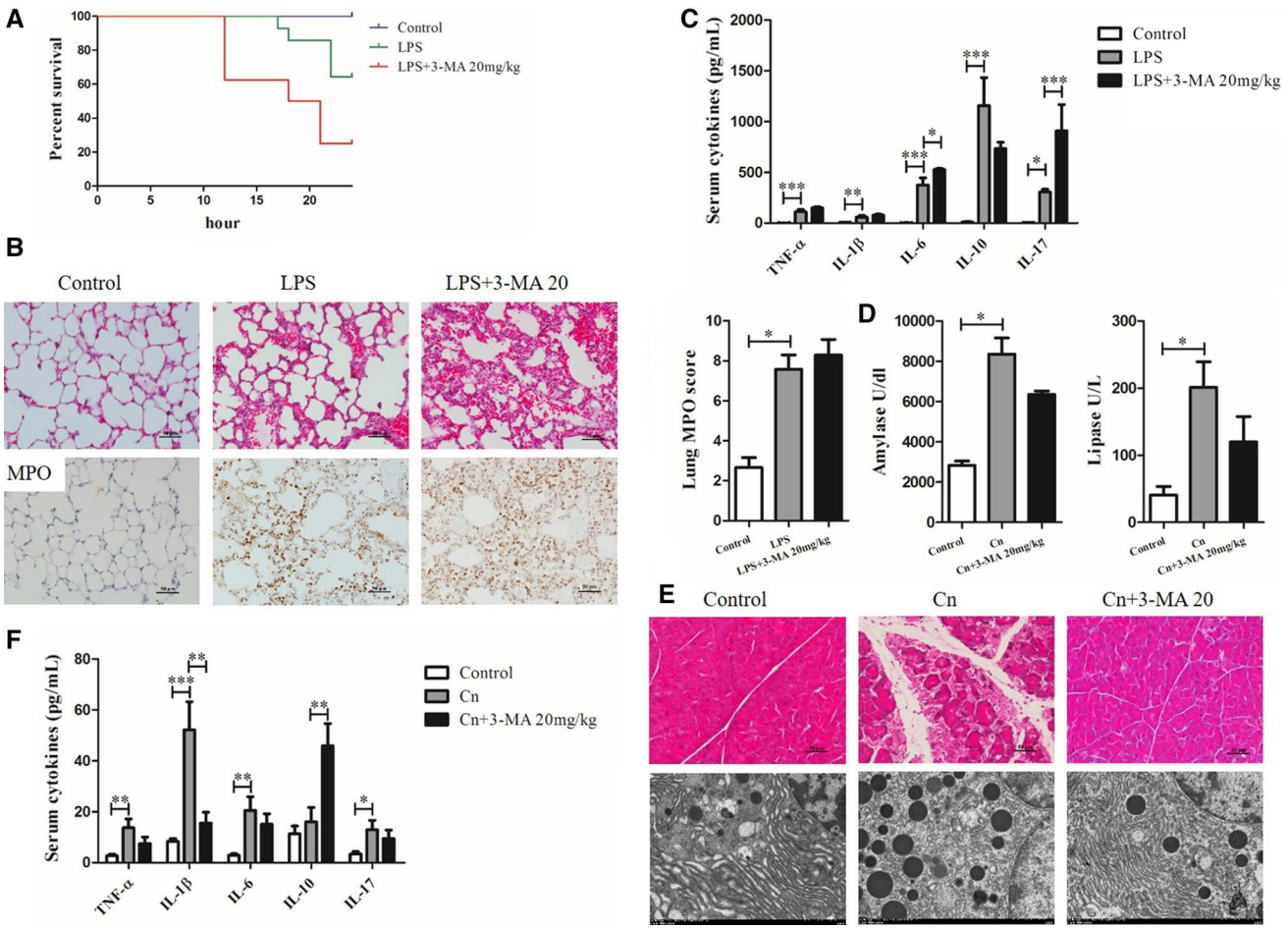

Fig. 5 3-MA treatment could not reduce the systemic inflammatory response induced by LPS but could significantly reduce the pancreatic injury induced by cerulein. **a** Survival rate of the LPS or LPS + 3-MA groups at different time points during the 24 h after the last LPS injection. **b** Histological analysis and immunohistochemical analysis of MPO revealed the damage and inflammation in the lung (×200). **c** ELISA revealed the effects of LPS or LPS + 3-MA treatment on the levels of serum TNF-α, IL-1β, IL-6, IL-10 and IL-17 (pg/mL). **d** Serum amylase (U/L) and serum lipase (U/L) activity in the Cn and Cn + 3-MA groups. **e** Histological analysis (×200) and TEM (×10,000) revealed the pathological damage and autophagic vacuoles in the pancreas, respectively. **f** ELISA revealed the effects of Cn or Cn + 3-MA groups on the levels of serum TNF-α, IL-1β, IL-6, IL-10 and IL-17 (pg/mL). Each value represents the mean ± standard deviation ($n = 8$–12 per group). $^{*}P < 0.05$, $^{**}P < 0.01$, and $^{***}P < 0.001$

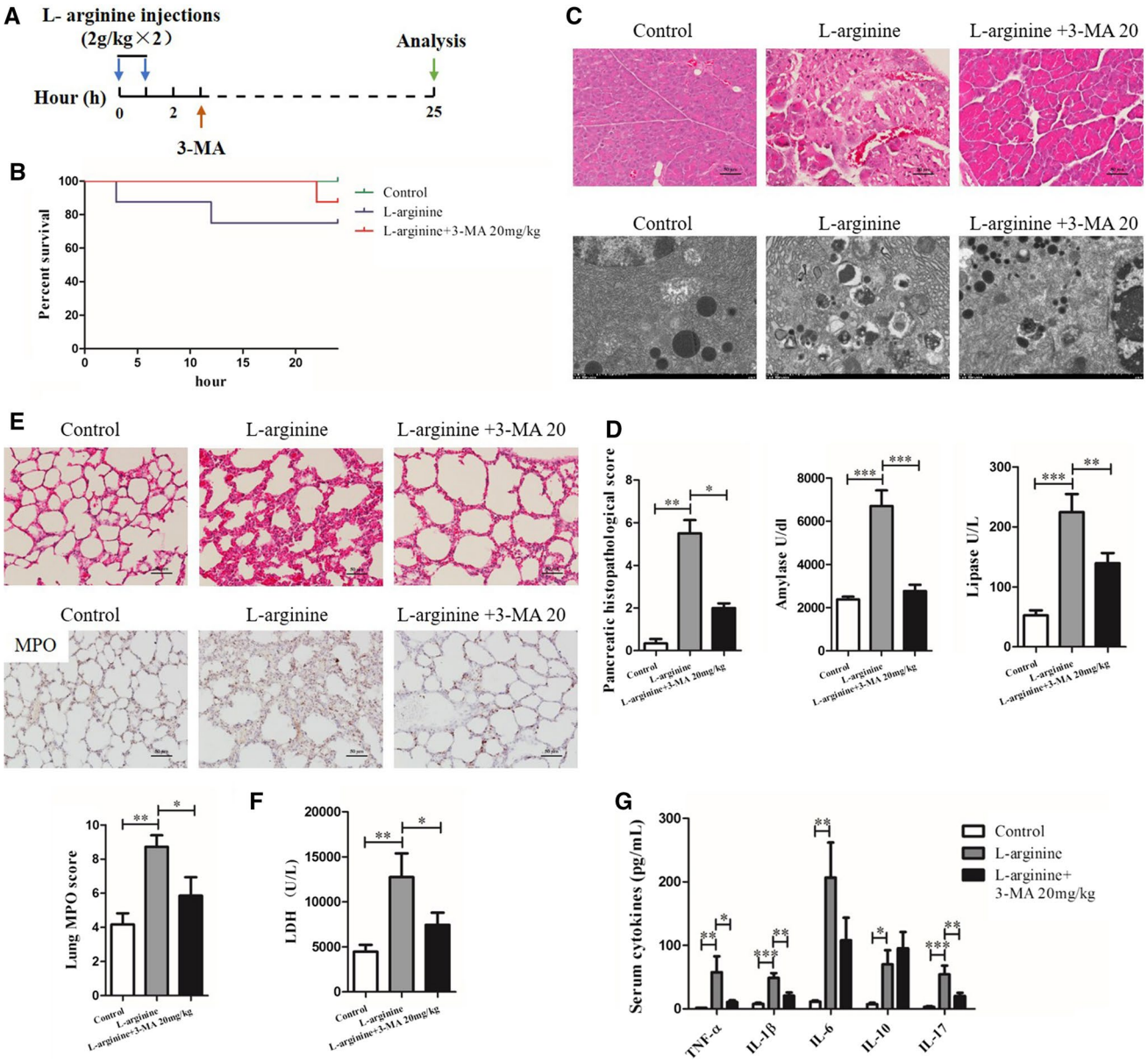

Fig. 6 Protective effects of 3-MA on SAP mice induced by L-arginine. **a** SAP was induced by a high dose of L-arginine (2 g/kg × 2) in BABL/c mice, and the autophagy inhibitor 3-MA (20 mg/kg) was intraperitoneally administered 2 h after the last injection of L-arginine. The mice were killed after anesthesia at 24 h after the last injection of L-arginine. **b** The survival rate of each group at different time points during the 24 h after the last injection of L-arginine. **c** Histological analysis (×200) and TEM (×10,000) revealed the pathological damage and autophagic vacuoles in the pancreas, respectively. **d** The histopathological score of pancreatitis severity, and serum amylase (U/L) and serum lipase (U/L) activity. **e** Histological analysis and immunohistochemical analysis of MPO revealed damage and inflammation in the lungs of L-arginine- or L-arginine + 3-MA-treated mice. **f** Serum LDH (U/L) activity in the L-arginine or L-arginine + 3-MA groups. **g** ELISA revealed the effects of L-arginine or L-arginine + 3-MA treatment on the levels of serum TNF-α, IL-1β, IL-6, IL-10 and IL-17 (pg/mL). Each value represents the mean ± standard deviation ($n = 8$–12 per group). $^{*}P < 0.05$, $^{**}P < 0.01$ and $^{***}P < 0.001$

mice, the expression of inflammatory cytokines, including TNF-α, IL-1β, IL-6, IL-10 and IL-17, was also significantly increased compared to the control mice, and IL-1β expression was also significantly increased compared to the cerulein + 3-MA mice ($P < 0.05$) (Fig. 5f).

Protective Effects of 3-MA on L-Arginine-Induced SAP Mice

SAP was induced by L-arginine administration as previously reported [7]. The inhibitor of autophagy, 3-MA, was intraperitoneally administered 2 h after the last injection

of L-arginine (Fig. 6a). The survival rate was lower in the L-arginine-induced SAP groups than in the L-arginine + 3-MA group (Fig. 6b). In the L-arginine group, necrosis, hemorrhage and inflammatory cell infiltration were observed (Fig. 6c). In the L-arginine + 3-MA group, pathological changes in the pancreas included minor edema of the glands (Fig. 6c). The percentage of autophagic vacuoles per cytoplasmic area was significantly reduced in the L-arginine + 3-MA group compared with the L-arginine group (Fig. 6c). The pathological score of the pancreas was significantly higher in the L-arginine group than in the L-arginine + 3-MA group ($P < 0.05$, Fig. 6d). The serum amylase and lipase content was significantly higher in the L-arginine group than in the L-arginine + 3-MA group ($P < 0.05$, Fig. 6d). The histological features of lung injury in the L-arginine group included more severe thickening of the alveoli and neutrophil infiltration than in the L-arginine + 3-MA group (Fig. 6e). The expression levels of MPO in the lung were significantly higher in the L-arginine group than in the L-arginine + 3-MA group (Fig. 6e). Serum LDH activity was significantly higher in the L-arginine group than in the L-arginine + 3-MA group ($P < 0.05$, Fig. 6f). The expression of inflammatory cytokines, including TNF-α, IL-1β, IL-6, IL-10 and IL-17, was also significantly increased in the L-arginine-induced mice compared to the control mice ($P < 0.05$) (Fig. 6g). The levels of IL-1β, IL-6 and IL-17 were significantly decreased in the L-arginine + 3-MA group compared to the L-arginine group ($P < 0.05$) (Fig. 6g).

Discussion

SAP is associated with high mortality and morbidity rates due to uncontrolled inflammatory progression and a poorly understood pathogenesis. Therefore, animal models were essential to advancing our understanding of the pathophysiological processes responsible for SAP. SAP mice were generated by the administration of a high dose of cerulein (100 μg/kg) plus LPS (5 mg/kg) in BABL/c mice; the SAP mice exhibited severe pathological changes in the pancreas and lungs, as described in previous research [6]. The combination of cerulein plus LPS induces more SAP than cerulein alone. LPS is an aggravating agent and impairs the local and systemic inflammatory response during acute experimental pancreatitis. In our study, the survival rate of this cerulein plus LPS model was only 64% (9/14), which is similar to that for SAP patients in the clinic [16]. Pancreatic pathology after SAP induction revealed obvious necrosis, and the presence of acute lung injury (ALI) also showed the severity of the lung injuries in this model. In a previous study, L-arginine-induced AP was associated with a different pancreatic necrosis rate depending on the mouse strain, and the L-arginine (2 × 4 g/kg IP)-induced BALB/c mice showed a relatively low rate of pancreatic necrosis (approximately 15%) [7]. Serum amylase and lipase activity and histological grading suggested that the L-arginine model of AP was successfully established in our study.

To maintain cellular homeostasis, autophagy degrades and recycles organelles as well as long-lived proteins through a lysosome-driven process, which plays a protective role against adverse environmental conditions. Autophagy controls inflammation through regulatory interactions with innate immune signaling pathways, by removing endogenous inflammasome agonists and through effects on the secretion of immune mediators [17]. Beclin-1 (the mammalian orthologue of the yeast protein ATG-6) and autophagy-related LC3 proteins (the mammalian paralogues of the yeast ATG-8 protein) are key regulators of phagophore formation [18]. During the phagophore closure process, cytosolic LC3-I is modified and becomes LC3-II, which is translocated to the membrane. P62/sequestosome 1 (SQSTM1), which can activate oxidative stress and NF-κB pathways if left to accumulate due to impaired autophagy, is specifically degraded through autophagy [19, 20]. Rapamycin specifically inhibits mTOR activity to induce autophagy [21], which also could effectively induce apoptosis and autophagy in pancreatic cancer cells [22]. 3-MA, a phosphatidylinositol 3-kinase (PI3 K) inhibitor, inhibits autophagy by preventing PI3 K-III from binding with beclin-1 to form autophagosomes [23]. To reduce the accumulation of autolysosomes, 3-MA, a commonly used early autophagy inhibitor, was used to treat experimental pancreatitis. AP is characterized by lysosomal/autophagic dysfunction and impaired autophagic flux manifested by a decreased rate of long-lived protein degradation as well as increased levels of LC3-II and p62 [3]. Impaired autophagy, inefficient protein degradation and defective cathepsin maturation impart features of a lysosomal disease to pancreatitis [24]. In the current study, the administration of 3-MA and RAPA significantly affected the severity of AP in cerulein plus LPS-induced mice, and the marker proteins of autophagy also showed corresponding changes. In response to inhibited autophagic flux by 3-MA, systemic and local injury was ameliorated, which suggests that 3-MA may be an effective therapeutic intervention. Xiao *et al*. reported that spautin-1, a well-documented, highly effective autophagy inhibitor, could reverse impaired autophagy to ameliorate AP and alleviate calcium overload in cerulein- or L-arginine-induced AP mice [25]. Similarly, hydrogen sulfide exacerbated taurocholate-induced AP by over-activating autophagy via the inhibition of mTOR [26]. At present, most compounds used to treat experimental pancreatitis are not yet suitable for clinical treatment of pancreatitis. Nevertheless, compounds for the treatment of experimental pancreatitis could prevent only post-endoscopic retrograde cholangiopancreatography (ERCP)

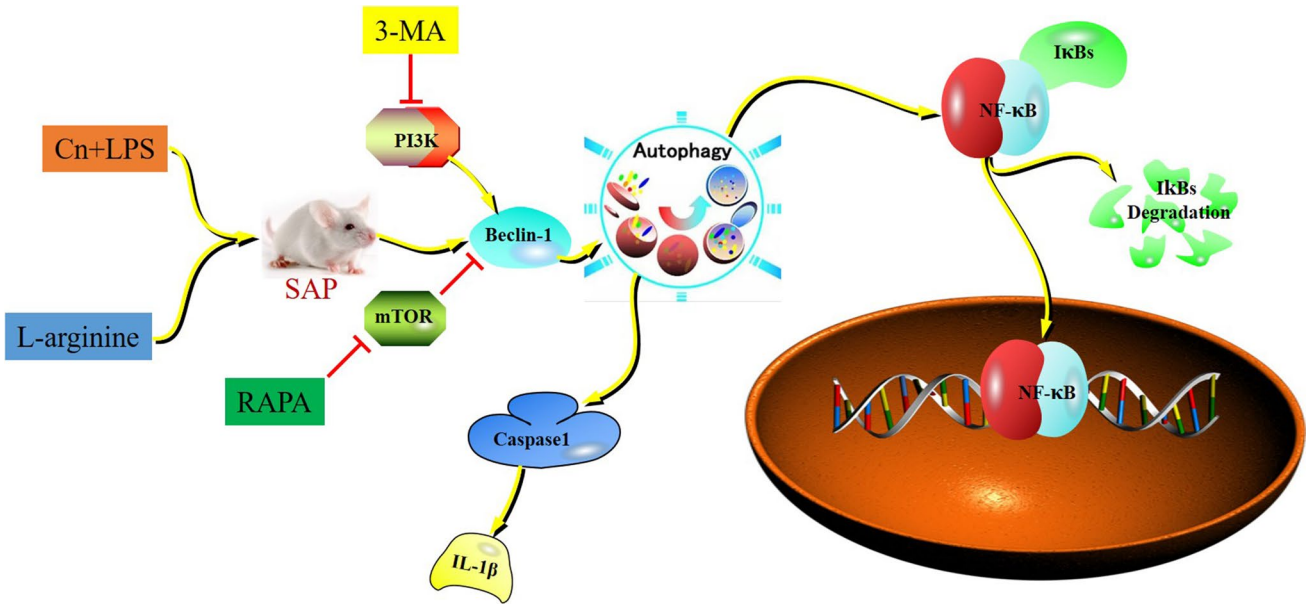

Fig. 7 The mechanism underlying the regulation of autophagy

pancreatitis, which is a common complication after ERCP. Therefore, choosing the 2 h after the last cerulein plus LPS injection time point may be more relevant to clinical treatment of pancreatitis. Acinar cell vacuolization in pancreatitis models is associated with decreased rates of degradation of long-lived proteins and the accumulation of p62, which indicate impaired autophagic flux. 3-MA, a commonly used early autophagy inhibitor, notably ameliorated the impaired autophagy in pancreatitis.

The nuclear factor κB (NF-κB) family, which consisted of five members, p65 (RelA), p50 (RelB), c-Rel, p105/p50 (NF-κB1) and p100/p52 (NF-κB2), plays a role in the regulation of inflammation, immunity, cell proliferation, differentiation and survival [27]. The p50/p65 heterodimer is the most common form in all cell types, and the activation of NF-κB causes the p50/p65 in the cytoplasm to translocate into the nucleus and bind specific DNA elements. IκB proteins are the main suppressor protein of NF-κB heterodimers; the most common isoform is IκBα. Recent studies have indicated that NF-κB activation is associated with most inflammatory diseases, including AP, in experimental models [28]. Specific knockdown or activation of NF-κB activity in AP confirms that NF-κB activity increases the severity of pancreatic inflammation, and the reduction in NF-κB activity may be used to treat patients with AP [29]. Wang et al. showed that both Acanthopanax and 3-MA may exert their therapeutic effects by inhibiting the PI3 K/Akt or NF-κB signaling pathways and inhibiting abnormal autophagy activation in pancreatic acinar cells [30]. In our study, 3-MA ameliorated the impaired autophagic flux to alleviate inflammation by modulating the NF-κB signaling pathway and caspase-1-IL-1β pathway, therefore decreasing injuries to the organs and the expression of inflammatory cytokines. Caspase-1 activated the production of cytokines IL-1β and IL-18, and its inhibition alleviates IL-1β-mediated lung and renal injuries in SAP rats [31, 32]. IL-1β is a pivotal initiating factor in SAP because it can induce the release of inflammatory cytokines. In lung tissue, LPS-induced lung damage leads to induced autophagy to reduce inflammation by removing accumulated ROS. However, treatment with 3-MA, an autophagy inhibitor, results in the accumulation of ROS and increased IL-1β secretion [33]. In our study, cerulein plus LPS treatment increased the degree of necrosis and inflammation in the pancreas, but obvious pancreatic pathology was not observed in the LPS-only group. Although the effect of 3-MA on non-autophagy-related anti-inflammatory activity is unclear, 3-MA may play a possible role, which is worth studying in the future.

The present study determined the role autophagy regulation using two models of SAP mice. The results showed that the inhibition of autophagy by 3-MA could significantly reduce the severity of pancreatitis pathology and improve prognosis, including the amelioration of injury in other organs. We also found that the amelioration of impaired autophagy could significantly reduce NF-κB signaling and the levels of serum cytokines. Our findings provide new insight into the role of autophagy regulation in the prognosis of SAP mice (Fig. 7). These data provided in our study show that ameliorating impaired autophagy by 3-MA treatment can be a potential therapy for SAP.

Acknowledgments This work was supported in part by the National Natural Science Foundation of China (No: 81460130), the Science and Technology Plan Grant (No. 20165092) from the Health Department of Jiangxi Province, China, and the Science and Technology Plan Grant (Key project) (No. GJJ160024) from the Education Department of Jiangxi Province, China.

Author's contribution LX and JW conceived and designed the experiments. DW, GH, YZ, YF, JW, TM, JN and GY performed the experiments. GH, XW, DW and RW analyzed the data. GH, XW and RW contributed reagents/materials/analysis tools. JW wrote the paper.

Compliance with ethical standards

Conflict of interest The authors declare that there are no conflicts of interest.

References

1. Forsmark CE, et al. Acute pancreatitis. *N Engl J Med*. 2016;20:1972–1981.
2. Lankisch PG, et al. Acute pancreatitis. *Lancet*. 2015;9988:85–96.
3. Gukovskaya AS, et al. Autophagy and pancreatitis. *Am J Physiol Gastrointest Liver Physiol*. 2012;9:G993–G1003.
4. Mareninova OA, et al. Impaired autophagic flux mediates acinar cell vacuole formation and trypsinogen activation in rodent models of acute pancreatitis. *J Clin Invest*. 2009;11:3340–3355.
5. Yang S, et al. Autophagy regulation by the nuclear factor kappaB signal axis in acute pancreatitis. *Pancreas*. 2012;3:367–373.
6. Wu D, et al. Reverse-migrated neutrophils regulated by JAM-C are involved in acute pancreatitis-associated lung injury. *Sci Rep*. 2016;6:20545.
7. Kui B, et al. New insights into the methodology of L-arginine-induced acute pancreatitis. *PLoS One*. 2015;2:e0117588.
8. Schmidt J, et al. A better model of acute pancreatitis for evaluating therapy. *Ann Surg*. 1992;1:44–56.
9. Wildi S, et al. Suppression of transforming growth factor beta signalling aborts caerulein induced pancreatitis and eliminates restricted stimulation at high caerulein concentrations. *Gut*. 2007;5:685–692.
10. He Z, et al. Intravenous hMSCs ameliorate acute pancreatitis in mice via secretion of tumor necrosis factor-alpha stimulated gene/protein. *Sci Rep*. 2016;6:38438.
11. Staubli SM, et al. Laboratory markers predicting severity of acute pancreatitis. *Crit Rev Clin Lab Sci*. 2015;6:273–283.
12. Minkov GA, et al. Pathophysiological mechanisms of acute pancreatitis define inflammatory markers of clinical prognosis. *Pancreas*. 2015;5:713–717.
13. Dai SR, et al. Serum interleukin 17 as an early prognostic biomarker of severe acute pancreatitis receiving continuous blood purification. *Int J Artif Organs*. 2015;4:192–198.
14. Denham W, et al. Gene targeting demonstrates additive detrimental effects of interleukin 1 and tumor necrosis factor during pancreatitis. *Gastroenterology*. 1997;5:1741–1746.
15. Petrov MS, et al. Organ failure and infection of pancreatic necrosis as determinants of mortality in patients with acute pancreatitis. *Gastroenterology*. 2010;3:813–820.
16. Banks PA, et al. Classification of acute pancreatitis–2012: revision of the Atlanta classification and definitions by international consensus. *Gut*. 2013;1:102–111.
17. Deretic V, et al. Autophagy in infection, inflammation and immunity. *Nat Rev Immunol*. 2013;10:722–737.
18. Mizushima N, et al. The role of Atg proteins in autophagosome formation. *Annu Rev Cell Dev Biol*. 2011;27:107–132.
19. Ichimura Y, et al. Pathophysiological role of autophagy: lesson from autophagy-deficient mouse models. *Exp Anim*. 2011;4:329–345.
20. Johansen T, et al. Selective autophagy mediated by autophagic adapter proteins. *Autophagy*. 2011;3:279–296.
21. Zeng X, et al. Mammalian target of rapamycin and S6 kinase 1 positively regulate 6-thioguanine-induced autophagy. *Cancer Res*. 2008;7:2384–2390.
22. Dai ZJ, et al. Antitumor effects of rapamycin in pancreatic cancer cells by inducing apoptosis and autophagy. *Int J Mol Sci*. 2012;1:273–285.
23. Katayama M, et al. DNA damaging agent-induced autophagy produces a cytoprotective adenosine triphosphate surge in malignant glioma cells. *Cell Death Differ*. 2007;3:548–558.
24. Gukovsky I, et al. Impaired autophagy underlies key pathological responses of acute pancreatitis. *Autophagy*. 2010;3:428–429.
25. Xiao J, et al. Spautin-1 ameliorates acute pancreatitis via inhibiting impaired autophagy and alleviating calcium overload. *Mol Med*. 2016;22:643.
26. Ji L, et al. Hydrogen sulphide exacerbates acute pancreatitis by over-activating autophagy via AMPK/mTOR pathway. *J Cell Mol Med*. 2016;12:2349–2361.
27. DiDonato JA, et al. NF-kappaB and the link between inflammation and cancer. *Immunol Rev*. 2012;1:379–400.
28. Jakkampudi A, et al. NF-kappaB in acute pancreatitis: Mechanisms and therapeutic potential. *Pancreatology*. 2016;4:477–488.
29. Rakonczay ZJ, et al. The role of NF-kappaB activation in the pathogenesis of acute pancreatitis. *Gut*. 2008;2:259–267.
30. Wang, X. *et al*. Acanthopanax versus 3-Methyladenine ameliorates sodium taurocholate-induced severe acute pancreatitis by inhibiting the autophagic pathway in rats. *Mediators Inflamm*, 8369704 (2016).
31. Zhang XH, et al. Caspase-1 inhibition alleviates acute renal injury in rats with severe acute pancreatitis. *World J Gastroenterol*. 2014;30:10457–10463.
32. Liu M, et al. Caspase inhibitor zVAD-fmk protects against acute pancreatitis-associated lung injury via inhibiting inflammation and apoptosis. *Pancreatology*. 2016;5:733–738.
33. Liu F, et al. MiR-155 alleviates septic lung injury by inducing autophagy via inhibition of transforming growth factor-beta-activated binding protein 2. *Shock*. 2017;48:61.